Level set based shape prior segmentation [*]

Tony Chan [†]   Wei Zhu [‡]

Abstract

In this paper, we propose a level set based variational method for segmentation using prior shapes. Inspired by Cremers' work [5], we also introduce a labelling function which together with the level set function for segmentation dynamically indicates the region with which the prior shape should be compared. Our model is capable of segmenting an object from an image based on the image intensity as well as the prior shape. In addition, the proposed model permits translation, scaling and rotation of the prior shape. Moreover, a fast way is also established for the minimization of our functional. The experiments validate our model.

1. Introduction

Segmentation is a fundamental topic in image processing. It is, in brief, a process that segments a given image into several parts in each of which the intensity is homogeneous.

Numerous approaches have been proposed for this problem. A fundamental one is Mumford-Shah's functional which is discussed comprehensively in [11]. In this approach, the segmentation problem is to find a piecewise smooth function which approximates the image and also prohibits the excessive length of the boundaries between any two contiguous regions. Due to the inconvenience to handle the length of the boundaries, a modified model which approximates Mumford-Shah's functional via $\Gamma-$ convergence was also developed. On the other hand, since the inception of level set methods by Osher and Sethian [12], they have become increasingly popular in many aspects because they could handle curves, surfaces with topological changes easily. Based on this method, Chan and Vese [2] proposed a novel, easily handled model for segmentation, which is exactly a piecewise constant case of Mumford-Shah's model. Besides these models, Caselles, et al. [1] developed a model that evolves an active contour which will be stable on the high gradient of intensities, i.e., the boundaries of objects.

However, all the above are all intensity based models. They will fail to segment meaningful objects when they are occluded by other ones or some parts of them are in low contrast even missing. In fact, these situations always happen in practical applications. This turns out that shape priors should be incorporated in the segmentation process.

There are also many works on shape priors segmentation in the literature. For example, in 2000, Leventon et al. [10] presented a statistical model which incorporates shape information into Caselles' geometric active contours model [1]. Later, by taking the same segmentation model, Chen et al. [4] proposed a variational model, and established the existence of the solution to the energy minimization. Moreover, in [7], Cremers et al. presented a statistical model by combining shape priors into Chan-Vese's model [2].

In a recent paper, Cremers et al. [5] proposed a variational approach in which, besides the level set function for segmentation, a new function called labelling function is introduced to indicate the regions in which shape priors should be enforced. By minimizing the proposed energy with respect to both the level set function and the labelling function, the approach could segment multiple independent objects and discriminate familiar objects from unfamiliar ones by means of the labelling function.

In this paper, based on Chan-Vese's model, we would like to propose a variational model for shape prior segmentation. In this model, we borrow the idea of Cremer's work in [5], i.e., we also introduce a labelling

---

[†]Department of Mathematics, University of California, Los Angeles, 405 Hilgard Avenue, Los Angeles, CA, 90095. E-mail: TonyC@college.ucla.edu

[‡]Department of Mathematics, University of California, Los Angeles, 405 Hilgard Avenue, Los Angeles, CA, 90095. E-mail: wzhu@math.ucla.edu

function. Basically, Our model differs from Cremer's in several aspects. Firstly, our approach permits scaling, translation and rotation of prior shapes. Secondly, we take a different shape comparison term which is intrinsic to the objects and the prior shapes, in other words, it is independent of the domain of the image. Moreover, we introduce more terms to control the labelling function.

The remainder of this paper is organized as follows. In section 2, a shape representation via a signed distance function is discussed. We utilize this shape representation in this paper. In section 3, we review some variational models on shape prior segmentation. Then, we detail our variational model in section 4. Section 5 contains the numerical algorithm and the experimental results are presented in Section 6, which is followed by a conclusion in section 7.

2. Shape representation via a signed distance function

In [13, 15], Paragios et al. represented a shape via a signed distance function – a special level set function [12]. Given an object $\Omega \subset R^2$, which is assumed to be closed and bounded, then there is a unique viscosity solution to the following equation:

$$| \nabla \phi |= 1$$

$$\phi \begin{cases} > 0 & x \in \Omega \backslash \partial \Omega \\ = 0 & x \in \partial \Omega \\ < 0 & x \in R^2 \backslash \Omega. \end{cases} \tag{1}$$

Hence, any object in the plane corresponds a unique signed distance function, and vice versa.

As a shape is invariant to translation, rotation and scaling, we may define an equivalent relation in the collection of objects in the plane. Any two objects are said to be *equivalent* if they have the same shape. Their signed distance functions are related. For example, let Ω_1 and Ω_2 be two objects with the same shape, and ϕ_1 and ϕ_2 be the signed distance functions respectively, then there exists a four-tuple (a, b, r, θ) such that:

$$\phi_2(x,y) = r\phi_1[\frac{(x-a)\cos\theta + (y-b)\sin\theta}{r}, \frac{-(x-a)\sin\theta + (y-b)\cos\theta}{r}], \tag{2}$$

where (a, b) represents the center, r the scaling factor and θ the angle of rotation. In this way, given any object, consequently a signed distance function, we may get the representation of other objects in the equivalent class by choosing the four-tuple (a, b, r, θ).

3. A review for shape prior segmentation

The literature on shape prior segmentation is vast, and an exhaustive survey is beyond the scope of this paper. We only review some variational frameworks which are related to our work.

3.1. Using prior shapes in geometric active contours (Chen et al.)

In [1], by extending the traditional energy-based active contours (snakes), Caselles et al. developed over a curve C an energy function $E(C)$, which reads:

$$\begin{matrix} min \\ C(q) \end{matrix} \int g(|\nabla I(C(q))|)|C'(q)|dq, \tag{3}$$

where $I : \Omega \to R$ be an image defined on Ω, and g is a function of the image gradient, usually it is of the form:

$$g(|\nabla I|) = \frac{1}{1 + |\nabla I|^2}. \tag{4}$$

By minimizing the energy $E(C)$, the curve C will be stable on the boundaries of objects in the image, where the gradients of intensity are very large.

In 2001, Chen et al. [4] developed a variational framework by incorporating shape priors into Caselles' model. They proposed a modified procrustes method to describe the shape priors. The method is as follows. Let C^* be

a curve, called *shape prior* , representing the boundary of an object, and C be another curve, then the difference between curve C and C^*, e.g., the two objects, is defined as:

$$\begin{array}{c} min \\ C(q) \end{array} \int d^2(\mu RC(q) + T)|C'(q)|dq, \tag{5}$$

where μ, R, T be the parameters for scaling, rotation and translation, and $d(x, y) = d(C^*, (x, y))$ is the distance from a point (x, y) to the curve C^*.

Then, by combining these two terms, Chen et al. proposed the energy for shape prior segmentation as:

$$E(C, \mu, R, T) = \int \{g(|\nabla I(C(q))|) + \frac{\lambda}{2}d^2(\mu RC(q) + T)\}|C'(q)|dq, \tag{6}$$

where $\lambda > 0$ is a parameter. Moreover, they choose $g(|\nabla I|)$ as:

$$g(|\nabla I|) = \frac{1}{1 + \beta|\nabla G_\sigma * I|}, \tag{7}$$

where $\beta > 0$ is a parameter, and $G_\sigma(x) = \frac{1}{\sigma}e^{-|x|^2/4\sigma^2}$.

This model can segment objects, whose shapes are similar to the prior ones, from images even when their complete boundaries are either missing or are low resolution and low contrast. Moreover, the model also provides the parameters of translation, rotation and scaling that map the active contour to the prior shape, which are useful in aligning images.

3.2. Segmentation using shape priors and dynamic labelling (Cremers et al.)

In [2], Chan and Vese proposed a variational model on a level set function, say ϕ, whose zero level set segments the image into several intensity homogenous regions. The functional reads:

$$E(c_1, c_2, \phi) = \int_\Omega \{(u - c_1)^2 H(\phi) + (u - c_2)^2(1 - H(\phi)) + \mu|\nabla H(\phi)|\}dxdy, \tag{8}$$

where $u : \Omega \to R$ is an image defined on Ω, c_1 and c_2 are two scalar variables, $H(x)$ is the Heaviside function as follows:

$$H(x) = \left\{ \begin{array}{ll} 1, & \text{x} \geq 0 \\ 0, & \text{x} < 0, \end{array} \right. \tag{9}$$

and $\mu > 0$ is a parameter which describes how large the length of the boundaries is permitted, since the term $\int_\Omega |\nabla H(\phi)|$ just represents the length of zero level set of ϕ.

Recently, Cremers et al. [5] developed a novel variational approach which incorporates shape priors into Chan-Vese's model. Besides the level set function ϕ, they introduced another function, called the *labelling* function, which will indicate the region where the shape prior should be enforced.

They adopted Paragios et al.'s method to represent a shape, that is, by means of a signed distance function (Reviewed in section 2). Let ϕ be the level set function for segmentation, and ϕ_0 be the one embedding a given shape. Both are signed distance functions. Then the shape difference reads:

$$E_{shape}(\phi) = \int_\Omega (\phi - \phi_0)^2 dxdy. \tag{10}$$

Clearly, this integral means that the shape prior is enforced on all the domain Ω, which will affect the segmentation of other objects and fail to segment the desirable object. Consequently, Cremers et al. introduced another function L, called *labelling* function, into the integral. The new shape term takes the form as:

$$E_{shape}(\phi, L) = \int_\Omega (\phi - \phi_0)^2(L + 1)^2 dxdy, \tag{11}$$

where L defines the parts of the image domain Ω where the shape prior should be active. For example, the region where $L = -1$ will be excluded from the integral.

As for controlling the area of the region on which the shape prior is enforced and the regularity of the boundary separating the regions, an integral shape prior is developed by Cremers et al. as:

$$E_{shape}(\phi, L) \quad = \quad \int_{\Omega} \{(\phi - \phi_0)^2 (L+1)^2 + \lambda^2 (L-1)^2 + \gamma |\nabla H(L)|\} dxdy. \tag{12}$$

In summary, Cremers et al.'s model is:

$$E(u_+, u_-, \phi, L) \quad = \quad E_{CV}(u_+, u_-, \phi) + \alpha E_{shape}(\phi, L), \tag{13}$$

where $\alpha > 0$ is a parameter.

In this paper, Cremers et al. also derived a way to simultaneously optimize the above energy with respect to the level set function ϕ and the labelling function L. For the detail, we refer to [5].

This idea that introducing a labelling function to indicate the region in which the shape prior is enforced is novel. Besides segmenting multiple independent objects in images, the model can also discriminate familiar objects, e.g., whose shapes are similar to the prior shapes, from unfamiliar ones by means of the labelling function. However, the above model does not permit the translation, rotation and scaling of the prior shape or the active contour.

4. Our Model

In this section, we will detail our model. In section 4.1, our model on shape prior segmentation for an image with only one object will be explained. Then in section 4.2, by introducing a labelling function, we will extend the model to general case that there are probably many objects in the image.

4.1. Shape prior segmentation for a simple case

Here, we will consider a simple case that there is only one object inside the given image.

Let $u : \Omega \to R$ be the given image defined on the domain Ω, ϕ a level set function for segmentation, and ψ a signed distance function for a given shape. As discussed in section 2, let ψ_0 be a fixed signed distance function for the shape, then ψ and ψ_0 are related by a four-tuple (a, b, r, θ) via the formula (2).

Instead of taking the shape comparison term as Cremers et al.'s in [5], we define it as follows:

$$E_{shape}(\phi, \psi) \quad = \quad \int_{\Omega} (H(\phi) - H(\psi))^2 dxdy, \tag{14}$$

where $H(x)$ is the Heaviside function as stated before. This term is symmetric to ϕ and ψ, and independent of the size of the domain Ω.

Therefore, our model for shape prior segmentation can be written as:

$$E(c_1, c_2, \phi, \psi) \quad = \quad E_{CV}(c_1, c_2, \phi) + \lambda E_{shape}(\phi, \psi), \tag{15}$$

where $\lambda > 0$ is a parameter.

Due to the relation (2) between ψ and ψ_0, we may also write the functional in terms of ψ_0 by replacing ψ with (a, b, r, θ).

We minimize the functional simultaneously with respect to ϕ and ψ (that is, the four-tuple (a, b, r, θ)). The numerical algorithm will be discussed in section 5.

4.2. Shape prior segmentation for general cases

As stated in section 4.1, the shape comparison term (14) is defined on all the domain. Hence, it is inapplicable to general cases that there are multiple objects inside the given image, since other objects will contribute to the shape comparison. In this section, our model for general cases will be stated.

Besides the segmentation function ϕ and shape function ψ, we also introduce one more level set function L, as called the *labelling* function in Cremers et al's work [5]. Then, the prior shape will be compared with the region

where both the level set function ϕ for segmentation and the labelling function L are positive. Consequently, instead of (14), the shape comparison term is defined as:

$$E_{shape}(\phi, L, \psi) \quad = \quad \int_\Omega (H(\phi)H(L) - H(\psi))^2 dxdy. \tag{16}$$

Here, $H(\phi)H(L)$ characterizes the intersection of $\{\phi > 0\}$ and $\{L > 0\}$. Ideally, the function L will segment from Ω a region inside which there is only the goal object.

Several conditions are needed to control the labelling function L. First, if $\{(x, y) \in \Omega : L(x, y) > 0\}$ is empty, the shape comparison term (16) will exert no effect on the segmentation process. Therefore, the region in which L takes positive value should be as large as possible. Second, the regularity should be required to the boundary where L separates the domain Ω by means of its zero level set.

Thus, we may rewrite the shape comparison term (16) as:

$$E_{shape}(\phi, L, \psi) \quad = \quad \int_\Omega (H(\phi)H(L) - H(\psi))^2 dxdy + \mu_1 \int_\Omega (1 - H(L))dxdy$$
$$+ \mu_2 \int_\Omega |\nabla H(L)| dxdy, \tag{17}$$

where $\mu_1 > 0$ and $\mu_2 > 0$ are two parameters. In this expression, the second term encourages the area of the region $\{(x, y) \in \Omega : L(x, y) > 0\}$, and the last one smoothes the boundary where L separates the domain Ω.

However, it is elusive to choose an appropriate μ_1. Too large μ_1 will impair the action of the labelling function because the region $\{L > 0\}$ will contain other objects besides the desirable object, and on the other hand, if it is so small, L could be stable at a state that the region $\{L > 0\}$ could be smaller than what it should be.

To overcome this dilemma, and notice that when the ideally segmentation for the goal object is obtained, the reference shape function ψ should also segment the object from the image, we introduce another term as:

$$E_\psi(\psi, c_1, c_2) \quad = \quad \int_\Omega \{(u - c_1)^2 H(\psi) + (u - c_2)^2 (1 - H(\psi))\} dxdy, \tag{18}$$

where c_1 and c_2 are the same variables in Chan-Vese's model. This term will be small when the desirable object is successfully segmented.

By combining all the above terms, our model can be written as:

$$E(\phi, \psi, L, c_1, c_2) \quad = \quad E_{CV} + E_{shape} + E_\psi, \tag{19}$$

or explicitly,

$$E(\phi, \psi, L, c) \quad = \quad \int_\Omega (u - c_1)^2 H(\phi) + (u - c_2)^2 (1 - H(\phi))$$
$$+ \lambda \int_\Omega (H(\phi)H(L) - H(\psi))^2$$
$$+ \mu_1 \int_\Omega (1 - H(L)) + \mu_2 \int_\Omega |\nabla H(L)|$$
$$+ \nu \int_\Omega (u - c_1)^2 H(\psi) + (u - c_2)^2 (1 - H(\psi)), \tag{20}$$

where $c = (c_1, c_2)$, and λ, μ_1, μ_2 and ν are nonnegative parameters.

Remark 1: In this functional, we omit the length term in E_{CV}. It is partially because that the prior shape may control the smoothness of ϕ to some extend, and on the other hand, without the length term, a fast way for minimizing the functional can be developed, which will be discussed in the following section. However, the length term can be included in the above functional if it is necessary, and then we will employ the conventional way to decrease the functional.

Remark 2: With the term E_ψ (18), the parameters μ_1 and μ_2 will be easy to choose. In fact, we fix them for all the experiments listed in this paper.

5. Numerical algorithm

In this section, we will discuss the numerical algorithms for minimizing the functionals presented in the last section. Moreover, we will develop a fast algorithm which is similar to Song and Chan's method [16].

5.1. Numerical algorithm for the simple case

Recall the functional (15):

$$E(c, \phi, \psi) = \int_\Omega (u - c_1)^2 H(\phi) + (u - c_2)^2 (1 - H(\phi))$$

$$+ \lambda \int_\Omega (H(\phi) - H(\psi))^2. \tag{21}$$

Here, we also omit the length term in the Chan-Vese's model.

Then, similarly as Chan-Vese's method in [2], the minimization of functional (21) is performed by solving the following equations (22)~(28):

$$c_1 = \frac{\int_\Omega u H(\phi) dx dy}{\int_\Omega H(\phi) dx dy}, \tag{22}$$

$$c_2 = \frac{\int_\Omega u (1 - H(\phi)) dx dy}{\int_\Omega (1 - H(\phi)) dx dy}, \tag{23}$$

and for the shape function ψ, the gradient descents with respect to the four-tuple (a, b, r, θ) are given as follows:

$$\frac{\partial a}{\partial t} = \int_\Omega (H(\psi) - H(\phi)) \{ \psi_{0x}(x^*, y^*) \cos \theta$$
$$- \psi_{0y}(x^*, y^*) \sin \theta \} \delta(\psi) dx dy, \tag{24}$$

$$\frac{\partial b}{\partial t} = \int_\Omega (H(\psi) - H(\phi)) \{ \psi_{0x}(x^*, y^*) \sin \theta$$
$$+ \psi_{0y}(x^*, y^*) \cos \theta \} \delta(\psi) dx dy, \tag{25}$$

$$\frac{\partial r}{\partial t} = \int_\Omega (H(\psi) - H(\phi)) \{ -\psi_0(x^*, y^*) + \psi_{0x}(x^*, y^*) x^*$$
$$+ \psi_{0y}(x^*, y^*) y^* \} \delta(\psi) dx dy, \tag{26}$$

$$\frac{\partial \theta}{\partial t} = \int_\Omega (H(\psi) - H(\phi)) \{ -r \psi_{0x}(x^*, y^*) y^*$$
$$+ r \psi_{0y}(x^*, y^*) x^* \} \delta(\psi) dx dy, \tag{27}$$

where ψ_0 is a fixed signed distance function representing the given shape, and ψ is related to ψ_0 via (2), and

$$x^* = \frac{(x - a) \cos \theta + (y - b) \sin \theta}{r},$$

$$y^* = \frac{-(x-a)\sin\theta + (y-b)\cos\theta}{r},$$

$$\psi_{0x} = \frac{\partial\psi_0}{\partial x}, \qquad \psi_{0y} = \frac{\partial\psi_0}{\partial y},$$

and for the segmentation function ϕ,

$$\frac{\partial\phi}{\partial t} = -\{(u-c_1)^2 - (u-c_2)^2$$
$$+2\lambda(H(\phi) - H(\psi))\}\delta(\phi), \qquad (28)$$

where $\delta(x)$ is the derivative of the Heaviside function $H(x)$ in the distribution sense. In the numerical experiments, as in Chan-Vese [2], we choose slightly regularized versions of them as follows:

$$H_\varepsilon(x) = \frac{1}{2}(1 + \frac{2}{\pi}\arctan(\frac{x}{\varepsilon})) \qquad (29)$$

and

$$\delta_\varepsilon(x) = \frac{1}{\pi}\frac{\varepsilon}{\varepsilon^2 + x^2}, \qquad (30)$$

where ϵ is always chosen to be proportional to the mesh size Δx.

In summary, for each iteration in the experiment, we can update c_1, c_2, ψ and ϕ one by one according to formulas $(22)\sim(28)$.

However, due to the fact that we only need the sign of segmentation function ϕ, we will update it instead of using formula (28) but the following principle:

$$\phi = \begin{cases} 1, & -\{(u-c_1)^2 - (u-c_2)^2 + 2\lambda(H(\phi) - H(\psi))\} \geq 0; \\ -1, & -\{(u-c_1)^2 - (u-c_2)^2 + 2\lambda(H(\phi) - H(\psi))\} < 0. \end{cases}$$
$$(31)$$

The principle will accelerate the minimization process remarkably. Similar methods can be found in several papers such as Song-Chan [16].

Below we will prove that this kind of principle is equivalent to the conventional method if we consider Chan-Vese's model without length term.

Theorem 1: *Let $u : \Omega \to R$ be a binary image defined on the domain Ω, for simplicity, denoted as $u = \chi_A(x, y)$, where χ_A is the characteristic function of $A \subseteq \Omega$, and $\phi : \Omega \times \{t \geq 0\} \to R$ be the segmentation function. Without length term, Chan-Vese's functional reads:*

$$E(c_1, c_2, \phi) = \int_\Omega \{(u-c_1)^2 H(\phi) + (u-c_2)^2(1 - H(\phi))\}dxdy,$$
$$(32)$$

the Euler-Lagrange equation for updating ϕ is:

$$\frac{\partial\phi}{\partial t} = -[(u-c_1)^2 - (u-c_2)^2]\delta(\phi), \qquad (33)$$

and c_1, c_2 are given by (22), (23). In this case, the principle (31) becomes:

$$\phi = \begin{cases} 1, & -[(u-c_1)^2 - (u-c_2)^2] \geq 0; \\ -1, & -[(u-c_1)^2 - (u-c_2)^2] < 0. \end{cases}$$
$$(34)$$

Then the minimization of this functional by performing (22), (23) and (33) will be the same as by performing (22), (23) and the principle (34).

Proof: For convenience, let us replace c_1, c_2 by $c_1(t)$, $c_2(t)$ in expressions (22),(23) and (33). And without loss of generality, suppose $c_1(0) > c_2(0)$, which are derived from (22) and (23) with the initial segmentation function $\phi(x, y, 0)$.

We claim that: by performing (22), (23) and (33), the term $(u - c_1(t))^2 - (u - c_2(t))^2$ will keep the sign.

In fact, the amount $(c_1(t) - c_2(t))^2$ will be non-decreasing as $t \to \infty$. This is because:

$$
\begin{aligned}
\frac{dc_1}{dt} &= \frac{(\int_\Omega u\delta(\phi)\phi_t)(\int_\Omega H(\phi)) - (\int_\Omega uH(\phi))(\int_\Omega \delta(\phi)\phi_t)}{(\int_\Omega H(\phi))^2} \\
&= \frac{1}{\int_\Omega H(\phi)}[\int_\Omega u\delta(\phi)\phi_t - c_1(t)\int_\Omega \delta(\phi)\phi_t] \\
&= \frac{1}{\int_\Omega H(\phi)}\int_\Omega (u - c_1(t))\delta(\phi)\phi_t \\
&= \frac{1}{\int_\Omega H(\phi)}\int_\Omega (u - c_1(t))\delta(\phi)[-(u - c_1(t))^2 + (u - c_2(t))^2]\delta(\phi),
\end{aligned}
\tag{35}
$$

then, if $c_2(t) < c_1(t)$, thus, $0 \leq c_2(t) < c_1(t) \leq 1$, it is easy to check that:

$$
(u - c_1(t))[-(u - c_1(t))^2 + (u - c_2(t))^2] > 0,
\tag{36}
$$

whenever u takes value 1 or 0. Therefore, $dc_1/dt \geq 0$. On the other hand, if $c_2(t) \geq c_1(t)$, we have $dc_1/dt \leq 0$. Consequently,

$$
(c_1(t) - c_2(t))\frac{dc_1}{dt} \geq 0,
\tag{37}
$$

similarly,

$$
(c_1(t) - c_2(t))\frac{dc_2}{dt} \leq 0.
\tag{38}
$$

Combining (37) and (38), we have:

$$
\frac{d(c_1(t) - c_2(t))^2}{dt} \geq 0,
$$

that is, the amount $(c_1(t) - c_2(t))^2$ is non-decreasing.

By the assumption, $c_1(0) > c_2(0)$, we may arrive that: $c_1(t) > c_2(t)$ for any $t > 0$. Consequently, the term $(u - c_1(t))^2 - (u - c_2(t))^2$ will keep the sign as $t \to \infty$.

Recall (33):

$$
\frac{\partial \phi}{\partial t} = -[(u - c_1)^2 - (u - c_2)^2]\delta(\phi).
$$

Since the right side will never change sign, i.e., the sign is the same as the sign of $-[(u - c_1(0))^2 - (u - c_2(0))^2]$. Therefore, if $-[(u - c_1(0))^2 - (u - c_2(0))^2] > 0$ at point $(x, y) \in \Omega$, $\phi(x, y, t)$ will be positive as $t \to \infty$, otherwise $\phi(x, y, t)$ will be negative as $t \to \infty$. This is just the principle (34). ♣

Remark : The theorem shows that it is reasonable to use the principle (31) to minimize the functional (21) to some extend. On the other hand, it will be unavoidable to view some fuzzy boundaries during the evolution if we apply the principle for very noise images. In this case, we prefer to use the conventional way with the length term.

5.2. Numerical algorithm for the general case

We now return to discuss the numerical algorithm for the functional (20). Similarly as discussed in the previous section, we update c_1, c_2, L, ψ and ϕ for each iteration in the experiments as follows:

$$c_1 = \frac{\int_\Omega u(H(\phi) + \nu H(\psi))dxdy}{\int_\Omega (H(\phi) + \nu H(\psi))dxdy}, \tag{39}$$

$$c_2 = \frac{\int_\Omega u((1 - H(\phi)) + \nu(1 - H(\psi)))dxdy}{\int_\Omega ((1 - H(\phi)) + \nu(1 - H(\psi)))dxdy}, \tag{40}$$

and

$$\begin{aligned}\frac{dL}{dt} &= -\lambda H(\phi)(1 - 2H(\psi))|\nabla L| + \mu_1|\nabla L| \\ &\quad + \mu_2|\nabla L|\nabla \cdot (\frac{\nabla L}{|\nabla L|}).\end{aligned} \tag{41}$$

As for the shape function ψ, we replace the term $(H(\psi) - H(\phi))$ in (24)~(27) by the following one:

$$2\lambda(H(\psi) - H(\phi)H(L)) + \nu[(u - c_1)^2 - (u - c_2)^2], \tag{42}$$

and

$$\frac{d\phi}{dt} = -\{[(u - c_1)^2 - (u - c_2)^2] + 2\lambda H(L)(H(\phi)H(\psi) - H(L))\}. \tag{43}$$

To speed up the minimization process, instead of (43), we update ϕ with the principle similar to (31), which reads:

$$\phi = \begin{cases} 1, & -\{[(u - c_1)^2 - (u - c_2)^2] + 2\lambda H(L)(H(\phi)H(\psi) - H(L))\} \geq 0; \\ -1, & -\{[(u - c_1)^2 - (u - c_2)^2] + 2\lambda H(L)(H(\phi)H(\psi) - H(L))\} < 0. \end{cases} \tag{44}$$

Moreover, we use local level set method, which was proposed by Peng et al. [14], to update the labelling function L, e.g., we only calculate L in a tube around its zero level set instead of the whole domain Ω. All these techniques make the minimization process much more faster than the conventional one. Generally, it always took 500 iterations for the experiments listed in this paper.

6. Experiment results

In this section, we only present experimental results for the general case (section 4.2) since the simple case (section 4.1) can be included in the general one. The experiments includes synthetic and real images. For the consistence and convenience for the choices of the parameters, we normalize the images by scaling them linearly from $[0, 255]$ to $[-1.0, 1.0]$.

6.1. Synthetic images

We report here two synthetic images: one is a triangle occluded by other objects (Figure 1) and the other is an incomplete triangle with missing part (Figure 2). The shape prior is the equilateral triangle.

To view the segmentation process clearly, we list three steps (initial, middle and final) for each function: segmentation function ϕ, labelling function L, shape function ψ and the goal segmentation, i.e., the zero level set of ϕ inside the domain where L takes positive value.

These two examples (Figure 1 and Figure 2) show that our model can combine intensity information and the prior shape prior to segment an object with a similar shape even though the object is occluded by other ones or some of its parts are missing.

9

6.2. Real images

In this section, we will apply our model to real images. We present here two images. One is a hand occluded by other objects (Figure 3) and the other is the same hand with some missing parts (Figure 4). The prior shape is a hand.

To get the signed distance function for the prior shape, we first apply Chan-Vese's segmentation model for the image with only a hand inside, then we obtain a level set function φ_0 which is positive inside the hand and negative outside the hand. Secondly, we solve a Hamilton-Jacobi equation as follows:

$$\frac{\partial \varphi}{\partial t} \;=\; sign(\varphi_0)(1 - |\nabla \varphi|) \tag{45}$$

to get a signed distance function φ. φ is the signed distance function corresponding to the hand, and defines the prior shape.

The examples (Figure 3 and Figure 4) listed here validate that our model is also capable of real images, that is, it can segment an object which is similar in shape to the prior one from an image even though the object is occluded by other ones or has some missing parts.

6.3. Discussion of our model

The difficulties of segmentation using shape priors lie primarily in several aspects.

Firstly, as shape priors are always employed as templates to supervise the segmentation process based on the intensities of images, which parts of regions should be affected by the templates? especially when there are other objects in images beside the desirable ones. This problem is discussed in this paper. As Cremers' work [5], we also introduce a labelling function to indicate with which part of segmentation the prior shape should be compared. Let's recall our model (20):

$$\begin{aligned}
E(\phi, \psi, L, c) \;=\; & \int_\Omega (u - c_1)^2 H(\phi) + (u - c_2)^2 (1 - H(\phi)) \\
& + \lambda \int_\Omega (H(\phi)H(L) - H(\psi))^2 \\
& + \mu_1 \int_\Omega (1 - H(L)) + \mu_2 \int_\Omega |\nabla H(L)| \\
& + \nu \int_\Omega (u - c_1)^2 H(\psi) + (u - c_2)^2 (1 - H(\psi)).
\end{aligned} \tag{46}$$

In this functional, the first line is Chan-Vese's model without length term; the following term measures the shape difference between the prior shape and the region encompassed by $\phi = 0$ and $L = 0$, i.e., the prior shape region $\psi > 0$ is compared with the region $\{\phi > 0\} \bigcap \{L > 0\}$, not $\{\phi > 0\}$; the remain terms in the last two lines describe how the labelling function L will evolve. In fact, it is insufficient for $\mu_1 \int_\Omega (1 - H(L))$ and $\mu_2 \int_\Omega |\nabla H(L)|$ to control the correct evolution of function L because too large μ_1 will make more segmentation region affected by the shape prior. Therefore, we add more terms as on the last line to mutually control the evolution of the labelling function L. In this way, the parameter μ_1, μ_2 are easy to handle. In fact, we fix them and vary only the parameters λ, ν in the experiments listed in this paper.

Secondly, how to choose the initial pose of the prior shape or shape template, i.e., in this paper, the shape function ψ? As many other methods, we put the initial prior shapes close to the desirable objects. However, this requirement still can not guarantee that the desirable objects can be segmented. For instance, in Figure (3) or (4), if the initial shape position of the hand is upside down, one can not expect the correct segmentation of the hand in the image, since the segmentation process could be trapped into a local minimum. Therefore, the initial position of the prior shape is crucial for the final result. We will explore this problem in the future.

7. Conclusion

We propose a level set based variational approach to incorporate shape priors into Chan-Vese's model for segmentation. In our model, besides the level set function for segmentation, as in Cremers' work [5], we introduce another

level set function together with the former one to mutually indicate with which region the prior shape should be compared. Our model can segment an object, whose shape is similar to the given prior shape which is independent of translation, scaling and rotation, from a background where there are several objects.

References

[1] V. Caselles, R. Kimmel and G. Sapiro, *Geodesic active contours,* International Journal of Computer Vision, 22:1, PP. 61-79, 1997.

[2] T. Chan and L.A. Vese, *Active contours without edges,* IEEE Transaction on Image Processing, 10(2):266-277, February 2001.

[3] T. Chan and L.A. Vese, *A level set algorithm for minimizing the Mumford-Shah functional in image processing,* In IEEE Workshop on Variational and Level Set Methods, pages 161-168, Vancouver, CA, 2001.

[4] Y. Chen, H. Tagare, S. Thiruvenkadam, F. Huang, D. Wilson, K. Gopinath, R. Briggs and E. Geiser, *Using prior shapes in geometric active contours in a variational framework,* International Journal of Computer Vision 50(3), 315-328, 2002.

[5] D. Cremers, N. Sochen, and C. Schnorr, *Towards recognition-based variational segmentation using shape priors and dynamic labeling,* In L. Griffith, editor, Int. Conf. on Scale Space Theories in Computer Vsion, volumn 2695 of LNCS, pages 388-400, Isle of Skye, 2003. Springer.

[6] D. Cremers and Stefano Soatto, *A Pseudo-distance for shape priors in level set segmentation,* N. Paragios(Ed.), 2nd IEEE Workshop on Variational , Geometric and Level Set Methods in Computer Vision, Nice, Oct 2003.

[7] D.Cremers, F. Tischhauser, J. Weickert, and C. Schnorr, *Diffusion snakes: introducing statistical shape knowledge into the Mumford-Shah functional,* Int. J. of Computer Vision, 50(3): 295-313, 2002.

[8] G. Kanizsa, *Organization in vision: essays on Gestalt perception,* Praeger, New York, 1979.

[9] M.E. Leventon, O. Faugeraus, W.L. Grimson and W.M. Wells III, *Level set based segmentation with intensity and curvature priors,* Mathematical Methods in Biomedical Image Analysis, 2000.

[10] M.E. Leventon, W.E. Grimson and O. Faugeraus, *Statistical shape influence in geodesic active contours.* Proc. IEEE Conf. Computer Vision and Patt. Recog., pp. 316-323.

[11] J.-M. Morel and S. Solimini, *Variational methods in image segmentation.* Birkhauser, Boston, 1995.

[12] S. Osher and J.A. Sethian, *Fronts propagating with curvature-dependent speed-algorithm based on Hamilton-Jacobi formulations,* J. Comput. Phys, Vol 79, 12-49, 1988.

[13] N. Paragios, M. Rousson and V. Ramesh, *Matching distance functions: A shape-to-area variational approach for global-to-local registration,* European Conference in Computer Vision, Copenhangen, Denmark, 2002.

[14] Danping Peng, Barry Merriman, Stanley Osher, Hongkai Zhao, and Myungjoo Kang, *A PDE-based fast local level set method,* J. Comput. Phys, Vol 155, 410-438, 1999.

[15] M. Rousson and N. Paragios, *Shape priors for level set representaions,* European Conference in Computer Vision, Copenhangen, Denmark, 2002.

[16] B. Song and T. Chan, *A fast algorithm for level set based optimization,* UCLA CAM Report 02-68, 2002.

[17] H.K. Zhao, *A fast sweeping method for Eikonal equations.*

[18] H.K. Zhao, T. Chan, B. Merriman and S. Osher, *A variational level set approach to multiphase motion.* J.Comput.Phys., 127:179-195,1996.

Original Image   Prior Shape

Initial

Middle

Final

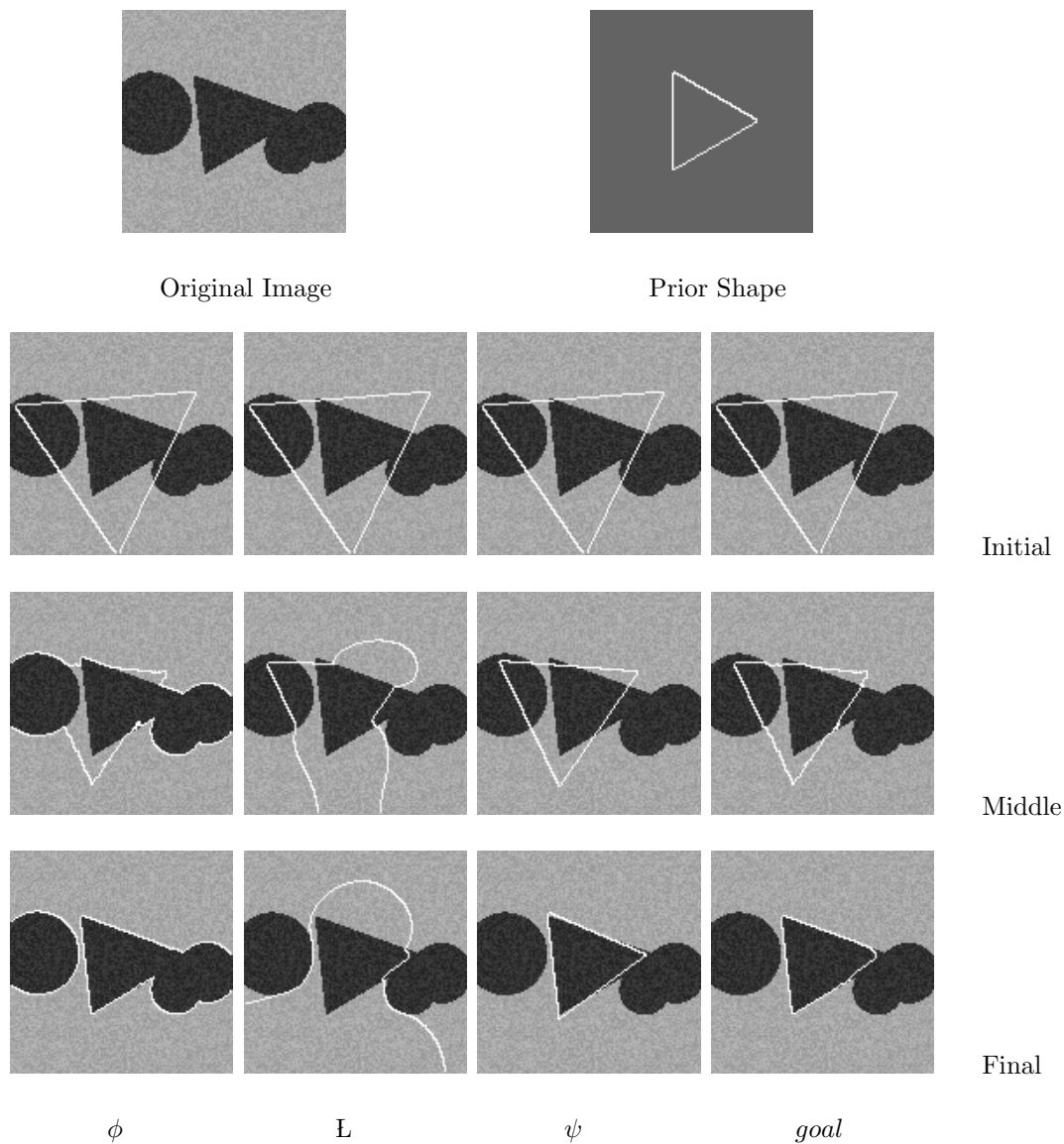ϕ Ł ψ *goal*

Figure 1: The first row lists the original image and the prior shape. From row 2 to row 4, each column respectively represents the initial, middle and final step of the segmentation function ϕ, labelling function L, shape function ψ, and the goal segmentation function whose zero level set is the just the one of ϕ inside the domain where L takes positive value. In this experiment, the parameters chosen are: $\lambda = 4.0$, $\mu_1 = 0.2$, $\mu_2 = 0.2$, $\nu = 2.0$. This example demonstrates that the model can segment the object, which is occluded by other ones and similar to the prior shape, out from a background with several objects.
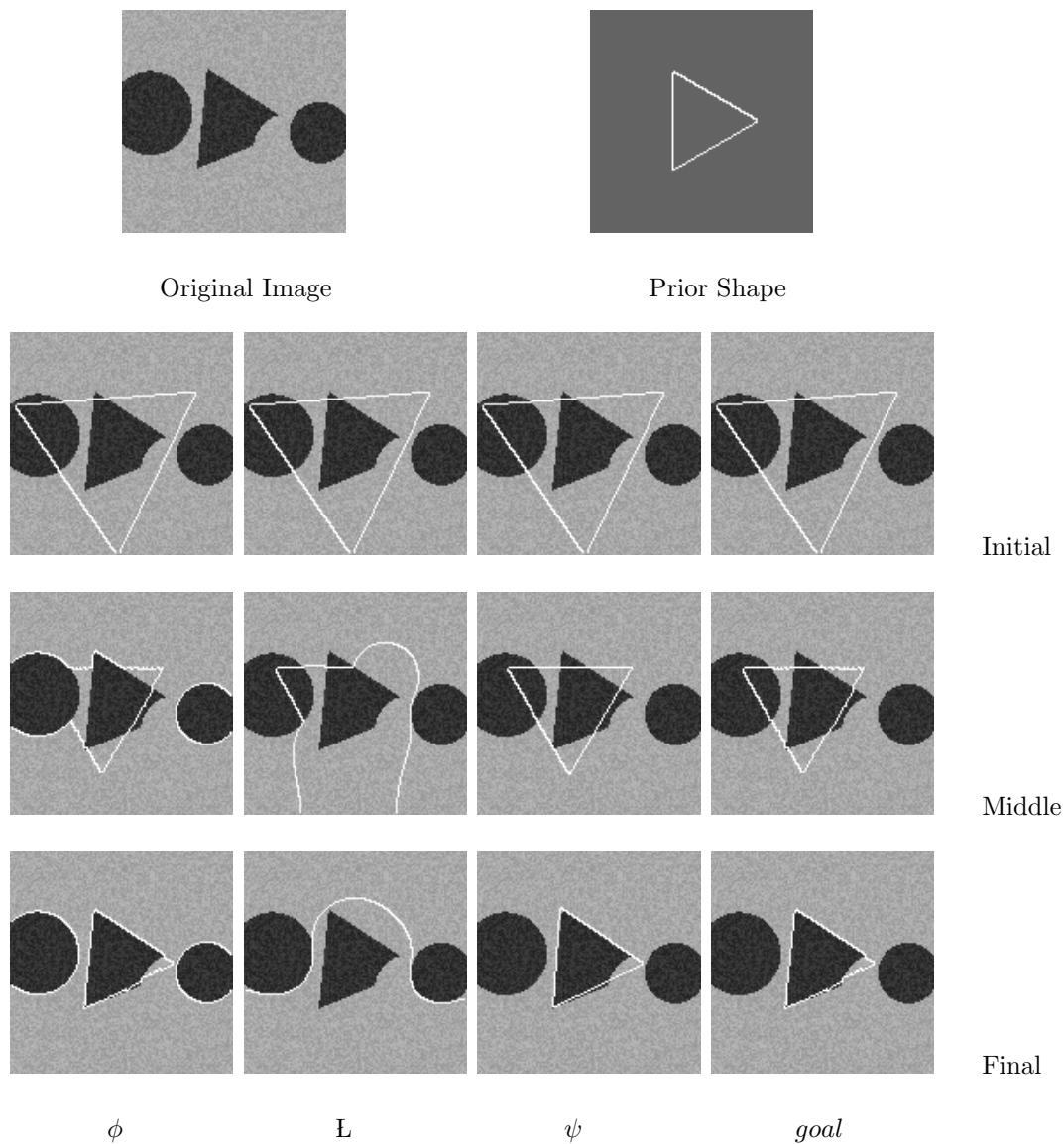
Figure 2: The first row lists the original image and the prior shape. From row 2 to row 4, each column respectively represents the initial, middle and final step of the segmentation function ϕ, labelling function L, shape function ψ, and the goal segmentation function whose zero level set is the just the one of ϕ inside the domain where L takes positive value. In this experiment, the parameters chosen are: $\lambda = 6.0$, $\mu_1 = 0.2$, $\mu_2 = 0.2$, $\nu = 0.5$. This example shows that our model is capable of capturing the object similar to the prior shape by filling in it missing parts from an image with several other objects.

Original Image   Prior Shape

Initial

Middle

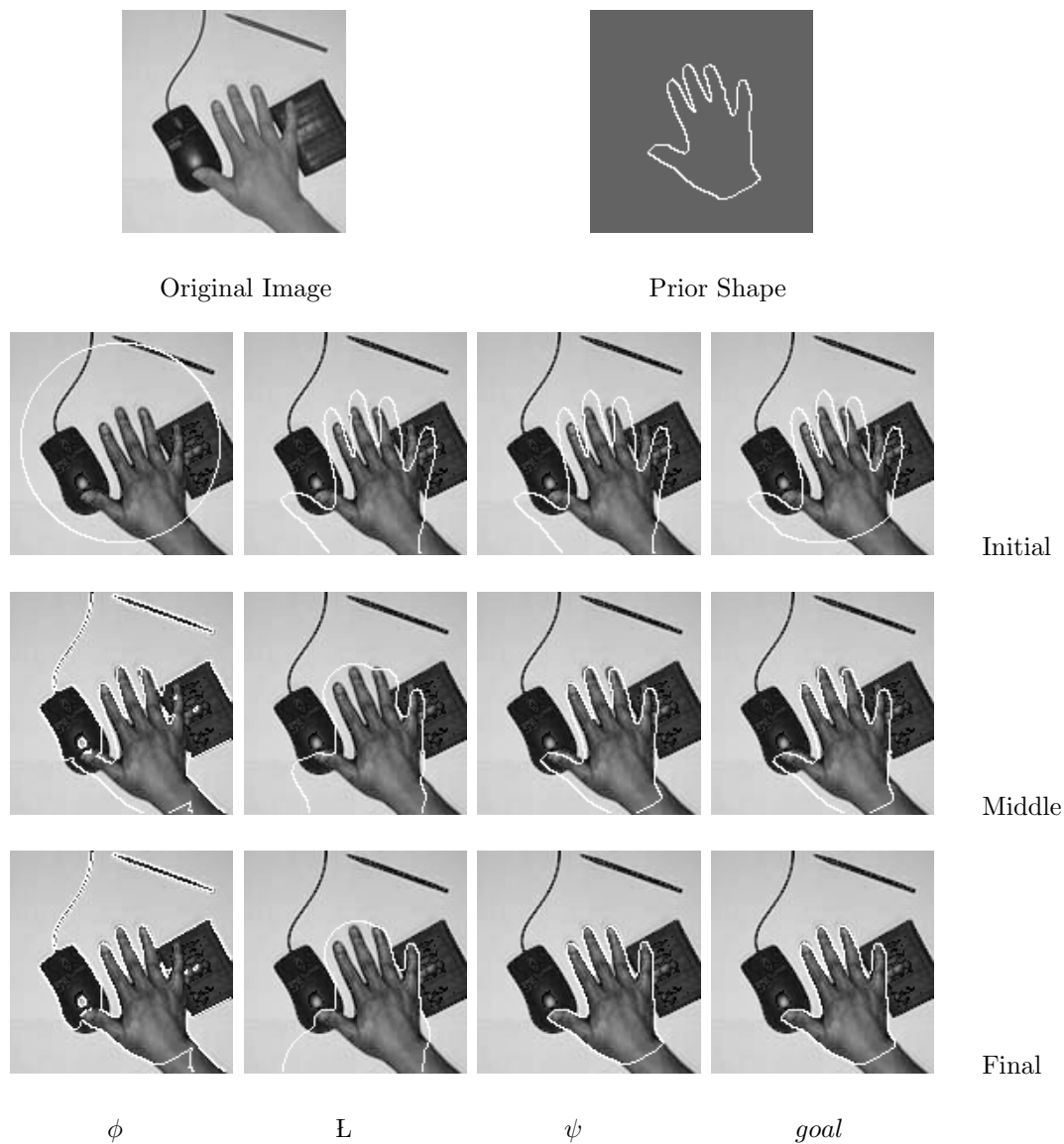Final

ϕ Ł ψ *goal*

Figure 3: The first row lists the original image and the prior shape. From row 2 to row 4, each column respectively represents the initial, middle and final step of the segmentation function ϕ, labelling function L, shape function ψ, and the goal segmentation function whose zero level set is the just the one of ϕ inside the domain where L takes positive value. In this experiment, the parameters chosen are: $\lambda = 3.0$, $\mu_1 = 0.2$, $\mu_2 = 0.2$, $\nu = 2.0$. This example verifies that our model can capture an object occluded by other ones via the supervision of the prior shape from a real image.
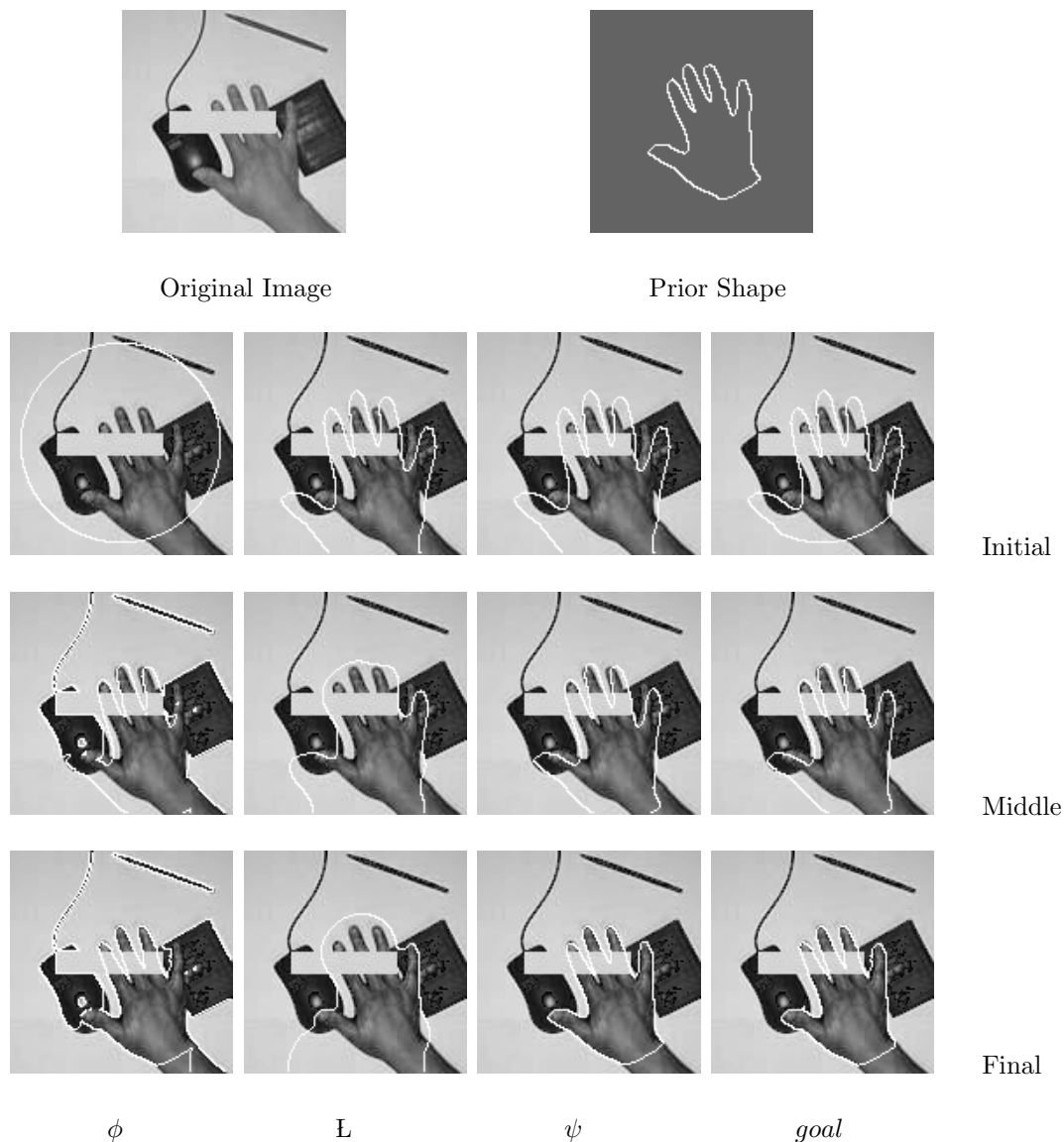
Figure 4: The first row lists the original image and the prior shape. From row 2 to row 4, each column respectively represents the initial, middle and final step of the segmentation function ϕ, labelling function L, shape function ψ, and the goal segmentation function whose zero level set is the just the one of ϕ inside the domain where L takes positive value. In this experiment, the parameters chosen are: $\lambda = 2.0$, $\mu_1 = 0.2$, $\mu_2 = 0.2$, $\nu = 2.0$. This example shows that our model can also be applied to segment an object similar to the prior shape by filling in the missing parts from a real image.